JOC The Journal of Organic Chemistry

Article

pubs.acs.org/joc

Photoredox-Assisted Reductive Cross-Coupling: Mechanistic Insight into Catalytic Aryl–Alkyl Cross-Couplings

Avishek Paul, Mark D. Smith, and Aaron K. Vannucci*

Department of Chemistry and Biochemistry, University of South Carolina, Columbia, South Carolina 29208, United States

Supporting Information

ABSTRACT: Here, we describe a photoredox-assisted catalytic system for the direct reductive coupling of two carbon electrophiles. Recent advances have shown that nickel catalysts are active toward the coupling of sp^3-carbon electrophiles and that well-controlled, light-driven coupling systems are possible. Our system, composed of a nickel catalyst, an iridium photosensitizer, and an amine electron donor, is capable of coupling halocarbons with high yields. Spectroscopic studies support a mechanism where under visible light irradiation the Ir photosensitizer in conjunction with triethanolamine are capable of reducing a nickel catalyst and activating the catalyst toward cross-coupling of carbon electrophiles. The synthetic methodology developed here operates at low 1 mol % catalyst and photosensitizer loadings. The catalytic system also operates without reaction additives such as inorganic salts or bases. A general and effective sp^2–sp^3 cross-coupling scheme has been achieved that exhibits tolerance to a wide array of functional groups.

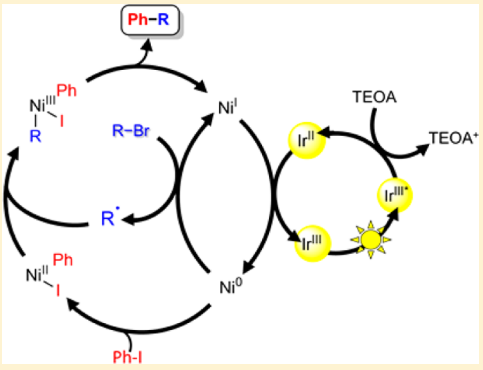

INTRODUCTION

Transition-metal-catalyzed carbon–carbon coupling reactions are of great importance for organic synthesis, the development of pharmaceuticals, total synthesis of natural products, and the electronics and chemical industries.[1−5] Advancements in the efficiency of cross-coupling reactions have been achieved in addition to the development of new methodologies for cross-coupling. A general comparison of the various methods for transition-metal-catalyzed C–C cross-coupling reactions is shown in Figure 1. Traditional coupling forms C–C bonds through the joining of a carbon electrophile with a carbon nucleophile. Selectivity for the cross-coupled product is inherent in this approach by the difference in reactivity between the electrophile and nucleophile; however, oxygen and moisture sensitivity of the carbon nucleophiles, kinetically slow transmetalation steps, and the need for highly reactive sp^3 carbon nucleophiles such as Grignard reagents are still challenges.[6] Additionally, strong bases are commonly employed to promote reactivity during transmetalation.[7]

To circumvent the challenges presented by the use of carbon nucleophiles in coupling reactions, the field of reductive C–C cross coupling, also referred to as cross-electrophile coupling,[8] removes the need for a carbon nucleophile and directly couples two carbon electrophiles. Carbon electrophiles, such as halocarbons, are more widely commercially available and typically more stable than their nucleophilic counterparts.[3] Furthermore, reductive couplings utilizing earth abundant nickel catalysts have exhibited remarkable reactivity with sp^3 carbons without detrimental β-hydride elimination side reactions that can occur with traditional coupling reactions catalyzed by more expensive palladium catalysts. Due to the similarity of the electrophilic substrates utilized in reductive coupling, selectivity for the cross-coupled product is not inherent. Dimerized substrate side products can decrease the yields of the desired cross-coupled product.

Generalized approaches to optimize cross-coupled products and avoid unwanted dimerization have been reported.[3,4,8] In fact, the many successful studies on selective reductive cross-couplings include the coupling of unactivated alkyl halides,[9−13] aryl halides,[14−16] pseudohalides,[12,17−19] asymmetric synthesis,[20−22] and detailed mechanistic understanding.[23,24] These reports use earth-abundant nickel catalysts; however, the reactions often require the use of heterogeneous reductants that require activation.[9] Reductive coupling reactions have also been achieved without the use of metal reductants[25,26] and through electrochemical processes.[27−29] In addition, chemical additives such as NaI, $MgCl_2$, and bases are commonly used to promote reactivity with the electrophile substrates.[6,9,11,15,21,30−32]

Photocatalytic cross-coupling offers another methodology that avoids the transmetalation step. Early reports on photoredox coupling catalysts illustrated the potential for sp^3–sp^3 coupling through two different routes for the formation of 1,2-diphenylethane.[33,34] More recently, catalytic schemes have been developed that combine iridium or ruthenium photoredox catalysts with nickel catalysts for cross-coupling reactions. In this process, the photoredox catalyst is excited by visible light and is then reductively quenched by one of the substrates, generating a substrate radical. The reduced photoredox catalyst then transfers

Received: November 27, 2016
Published: January 23, 2017

DOI: 10.1021/acs.joc.6b02830
J. Org. Chem. 2017, 82, 1996–2003

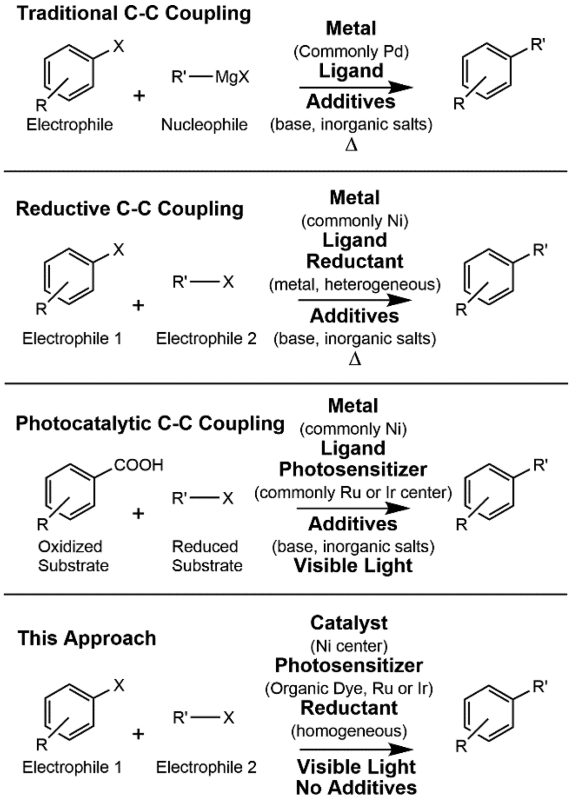

Figure 1. Representative approaches to transition-metal-catalyzed cross-coupling. X = halogen.

an electron to a second nickel catalyst. The second catalyst then reduces a second substrate and aids in the cross-coupling of the two substrates.[35−37] This catalytic approach has successfully coupled a variety of sp^2−sp^3 and sp^3−sp^3 C−C, C−N, and C−O products[38−44] and tends to exhibit good functional group tolerance. However, the requirement of one of the substrates to reductively quench the photoredox catalyst may limit the choice of possible coupling partners.

This report further develops and utilizes photoredox-assisted reductive cross-coupling (PARC) for C−C cross-coupling. The methodology of PARC offers advantages by combining the use of photoredox reactivity, sustainable visible light, and the chemistry of reductive cross-coupling. As opposed to previous studies, this system does not require stoichiometric amounts of heterogeneous reductants such as Zn or Mn. The PARC system instead uses a photosensitizer, the low-redox potential (E_{red} = −0.35 V), homogeneous, reductant triethanolamine, and sunlight to reduce the catalyst and drive the reductive-coupling catalytic cycle. The use of an amine reductant is advantageous in this system because it also promotes reactivity of the halides.

Very recently, two studies were published that showed photoredox-assisted reductive coupling was capable of sp^2−sp^3 cross-coupling. In the first study by the MacMillan group, light-drive cross-electrophile coupling was achieved with addition of a silane and a base instead of triethanol amine.[45] In this study, a silyl radical is generated in situ via reaction between the added silane and base. The resulting silyl radical was then capable of generating alkyl radicals from alkyl halides. The alkyl radicals were coupled to aryl halides through a Ni catalyst that was activated by visible light and an iridium chromophore. In the second report, a study more analogous to this report, the Lei group utilized a Ni catalyst and an Ir photosensitizer in 10 and 1 mol % loadings, respectively, to couple aryl halides with alkyl halides.[46] Using visible light, a triethylamine reductant, and 1.0 equiv of $MgCl_2$ additive led to cross-coupled yields up to 86%.

With the catalytic system reported in this paper, we offer further support for photoredox reductive coupling. Our system uses 1 mol % of Ni catalyst and Ir photosensitizer loading without any additives to achieve a variety of aryl−alkyl cross-coupled products. In addition, the triethanolamine reductant plays two roles in the cycle by also complexing halide leaving groups, which promotes halocarbon reactivity, eliminates the need for reaction additives, and aids in product separation.

RESULTS AND DISCUSSION

PARC System. The components of our photoredox-assisted reductive cross-coupling (PARC) system, a photosensitizer (**PS**), a Ni catalyst (**Cat**), and triethanolamine (TEOA) are depicted in Figure 2. Previous reports have shown nickel

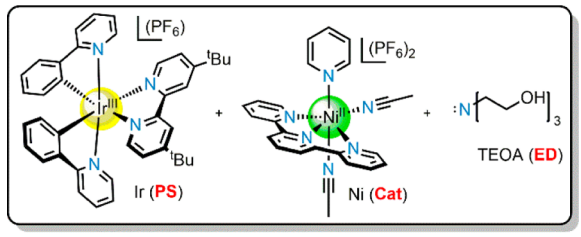

Figure 2. Components of the catalytic photoredox-assisted reductive cross-coupling (PARC) system.

complexes containing substituted terpyridine ligands are efficient for C−C coupling reactions;[14,30] however, nickel complexes containing unsubstituted terpyridine have shown limited solubility in organic solvents and hence have not been widely studied as cross-coupling catalysts.[47] To increase the solubility of the Ni−terpyridine moiety, an excess of pyridine (py) was added to a suspension of [Ni(tpy)Cl]Cl in ethanol (tpy = 2,2′:6′,2″-terpyridine). Subsequent addition of excess acetonitrile followed by addition of NH_4PF_6 resulted in a precipitate that was found to be soluble in a variety of organic solvents including acetonitrile. Acetonitrile proved to be the ideal solvent for increasing the ease of separating the organic products and TEOA salts from the reaction mixture. Crystallographic characterization of the nickel catalyst revealed a six-coordinate nickel center containing tpy, one py, and two acetonitrile ligands in the coordination sphere (Figure S30).

Cyclic voltammetry was used to determine the redox characteristics of the Ni catalyst. In acetonitrile, the catalyst exhibited two separate, one-electron quasi-reversible reductions at $E_{1/2}$ = −1.06 V and $E_{1/2}$ = −1.72 V versus the ferrocenium/ferrocene (Fc^+/Fc) couple (Figure S2). The quasi-reversibility of the reductions ($\Delta E_p \approx 120$ mV) is likely due to the lability of the pyridine and acetonitrile ligands but also signifies that the Ni(tpy) unit maintains structural integrity, even in a highly reduced redox state. Previous experimental and computational investigations on Ni^I(tpy)X, where X = Br^- or CH_3^-, indicated that reductions can occur either at the nickel center or the tpy ligand depending on the identity of the X ligand.[47] For the case of our nickel catalyst, a Ni(II) oxidation state exists in the ground state; therefore, the first reduction is assigned to the Ni(I)/Ni(II) redox couple. The exact nature of the second reduction has not yet been determined; however, electrochemical investigations discussed in further detail later in the manuscript, indicated that a

DOI: 10.1021/acs.joc.6b02830
J. Org. Chem. 2017, 82, 1996−2003

doubly reduced catalyst is necessary to initiate catalytic coupling reactions.

To generate a doubly reduced Ni complex in a photoredox-assisted system, a photosensitizer with the proper reductive driving force is required. Therefore, the iridium-based chromophore $[Ir(ppy)_2(tbpy)](PF_6)$ (**PS**), where ppy is 2-phenylpyridine and tbpy is 4,4′-di-*tert*-butyl-2,2′-dipyridine, was chosen. The Ir(II)/Ir(III) potential of **PS** at $E_{1/2} = -1.87$ V vs Fc^+/Fc gives roughly 0.15 V of thermodynamic driving force to generate the fully reduced Ni catalyst. To complete the catalytic system, the commercially available electron donor triethanolamine (TEOA) was utilized as the electron source to reductively quench **PS** upon visible-light photoexcitation.

Catalytic Homocoupling of sp^3 Halocarbons. To gain an understanding of the reactivity of the catalytic system, reaction conditions were initially screened for the homocoupling of 1-bromohexane in acetonitrile. Using a white light source, just 1.0 mol % of **PS**, 1.0 mol % of **Cat**, and 2.5 equiv of TEOA, a yield of 96% of the dimerized dodecane product was obtained in 12 h. Initially an unfiltered white light source was utilized, which resulted in lower product yields (<50%) likely due to decomposition of **Cat** and **PS**. Filtering off the high energy UV and near-UV light using a long-pass 400 nm cutoff filter resulted in much greater product yields. No product was detected if any components of the catalytic system, **PS**, **Cat**, or TEOA, were removed (Scheme 1), indicating that each component of the

Scheme 1. Control Experiments Showing All Three Components Are Necessary for Coupling of Alkyl Halides

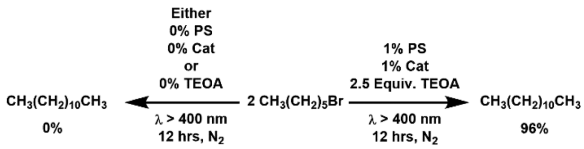

catalytic system is essential and that the nickel catalyst is directly involved in the coupling reaction. Increasing the amount of TEAO to 5.0 eqs did not result in increased catalytic activity. Additionally, only a 28% yield of product was detected when the Ir photosensitizer was replaced with $Ru(bpy)_3^{2+}$, where bpy is 2,2′-bipyridine. The similarity between the Ru(I)/Ru(II) redox couple of −1.76 V vs Fc^+/Fc and the second reduction potential of **Cat** (−1.72 V vs Fc^+/Fc) leads to inefficient electron transfer from the Ru chromophore to the catalyst and hence decreased catalytic activity.

Utilizing the optimized reaction conditions, the homocoupling of a series of unactivated alkyl halides was investigated to develop an understanding of the reactivity of the catalytic system.[30,48] Table 1 shows that good to excellent yields were obtained in nearly all cases. The straight-chain brominated alkyls, 1-bromobutane and 1-bromohexane, successfully coupled with excellent yields of 95% and 96%, respectively (reactions 2 and 5). The chloro analogue, 1-chlorohexane, did not exhibit coupling reactivity, however (reaction 1). The iodo analogue, 1-iodohexane, was expected to show equal or greater reactivity than the brominated alkyls due to previously reported results;[30] however, as entries 3 and 4 in Table 1 show, homocoupling of 1-iodohexane was kinetically slower and the reaction required 24 h to fully consume the substrate. Formation of I_2 during the reaction, confirmed by UV−vis spectroscopy (Figure S3), likely interfered with light absorption by PS. Light-driven formation of

Table 1. Photoredox-Assisted Reductive Coupling of Alkyl Halides[a]

#	R-X	R-R	% Yield[b]
1	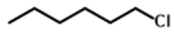		0
2	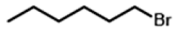		96
3			67
4			98[c]
5			95
6	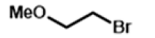		95
7	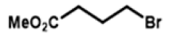		98
8	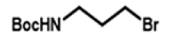		85
9			90
10	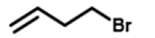		98
11	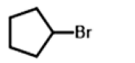	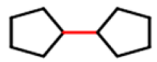	96
12	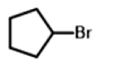		30[d]

[a]R−X = 0.32 mmol; **PS** = 0.0032 mmol; **Cat** = 0.0032 mmol; TEOA = 1.6 mmol in 4 mL of acetonitrile under N_2. White light irradiation of $\lambda \geq 400$ nm for 12 h with stirring. [b]Isolated yields, product determination via NMR compared to NIST database when available. [c]24 h. [d]$[Ru(bpy)_3](PF_6)_2$ used instead of PS.

halogens from halides utilizing transition-metal chromophores has been previously reported.[49]

This catalytic system also exhibited functional group tolerance in the homocoupling of alkyl halides. Efficient dimerization was achieved with substrates containing methoxy (95%, reaction 6), methoxycarbonyl (98%, reaction 7), and *tert*-butoxycarbonyl protected amine (85%, reaction 8). Functional group tolerance was also exhibited for strong electron-withdrawing groups (CF_3, 90%, reaction 9) and vinyl groups (98% reaction 10). The secondary bromide, cyclopentyl bromide, was also successfully dimerized (96%, reaction 11).

Catalytic Cross-Coupling Reactions. The PARC method exhibited good yields with low catalyst loadings for the dimerization of unactivated alkyl halides; however, dimers are typically unwanted side products in reductive cross-coupling reactions. With the goal in mind of showing PARC is capable of efficient cross-coupling catalysis, we also examined the reactivity of our catalytic system toward sp^2-carbon electrophiles. Under identical conditions that led to the dimerization of alkyl halides, little-to-no dimerization of iodobenzene was observed (Scheme 2), and GC−MS analysis only showed remaining starting material. This result indicates that sp^2 and sp^3 electrophiles undergo different reactivity with the nickel catalyst, as has been previously reported.[3,10]

Utilizing the optimized reaction conditions and knowing that the system reacts differently to sp^2 and sp^3 halides, we examined the capability of the PARC system to perform aryl-alkyl cross-

DOI: 10.1021/acs.joc.6b02830
J. Org. Chem. 2017, 82, 1996−2003

Scheme 2. Reaction Showing the Lack of sp^2–sp^2 Coupling from the Catalytic System

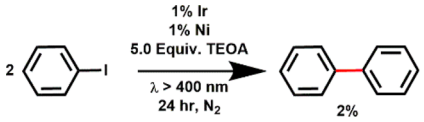

coupling reactions. A small excess of the aryl halide was required to help prevent dimerization of the sp^3 carbon electrophiles, as has been observed in related coupling schemes.[15] As Figure 3

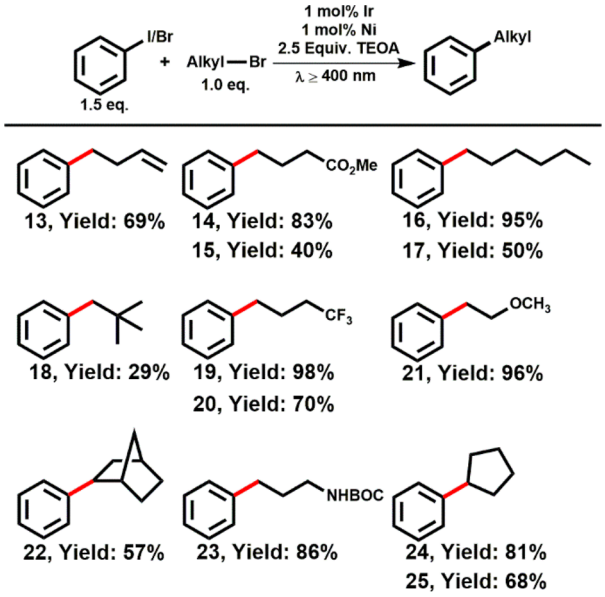

Figure 3. PARC of alkyl bromides with iodobenzene. Alkyl-Br = 0.32 mmol; **PS** = 0.0032 mmol; **Cat** = 0.0032 mmol; TEOA = 0.4 mmol in 4 mL of acetonitrile under N_2. White light irradiation of $\lambda \geq 400$ nm for 12 h. Products with two reaction numbers and yields are different with respect to the starting aryl halide, with the first reaction number corresponding to iodobenzene and the second reaction number corresponding to bromobenzene. Isolated yields and % yields based on limiting reagent.

shows, this PARC system is efficient in the coupling of alkyl-bromides with iodobenzene. Control experiments where one of the components of the catalytic system were removed once again resulted in no products being formed. In addition, reactions performed with $NiCl_2$, terpyridine, and pyridine in a 1:1:1 ratio instead of using the presynthesized catalyst resulted in decreased product yield to 40% for reaction 16, with alkyl–alkyl and aryl–aryl dimers also being identified as products (Table S2).

Further examination into Figure 3 shows that PARC once again exhibits functional group tolerance during efficient cross-coupling reactions. Substrates containing alkene functionalization (84%, reaction 13), methoxycarbonyl- (83%, reaction 14), methoxy- (96%, reaction 21), or *tert*-butoxycarbonyl-protected amine (86%, reaction 23), or an electron-withdrawing substituent (trifluoromethyl 98%, reaction 19) all resulted in high product yields. Cross-coupling between iodobenzene and neopentyl bromide (reaction 18) resulted in low yields likely due to the increased steric demands of the bromide. In addition, tertiary halides were not successfully coupled. Secondary alkyl bromides, however, were involved in high-yield cross-couplings (reaction 22, 72%, and reaction 24, 81%). Substituting bromobenzene in place of iodobenzene led to slightly diminished yields of the cross-coupled products (reactions 15, 17, 20, and 25), indicating kinetically facile reaction with the aryl halide is necessary to avoid dimerization of the alkyl halide substrates. GC–MS analysis of the reaction mixtures indicated that the only side products observed in the cross-coupling reactions were alkyl–alkyl dimers. For the case of reaction 18, alkyl halide starting material was also detected.

The substrate scope for this PARC system was then expanded to a range of substituted aryl halides. Table 2 shows that aryl

Table 2. PARC Reactions between Aryl Halides and Bromobutane[a]

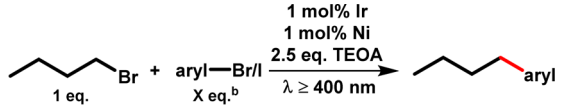

#	Product (starting halide)	% Yield[c]
26	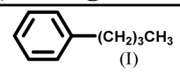	80
27	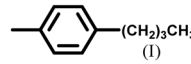	96
28	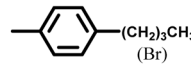	85
29	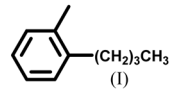	20
30	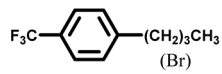	96
31	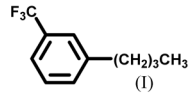	91
32	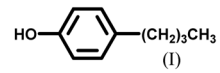	95
33	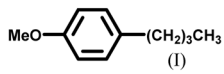	83
34	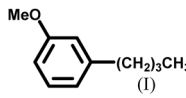	78
35	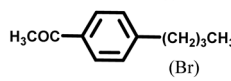	92
36	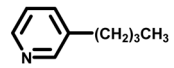	75

[a]Bromobutane = 0.32 mmol; **PS** = 0.0032 mmol; **Cat** = 0.0032 mmol; TEOA = 0.4 mmol in 4 mL of acetonitrile under N_2 for 18 h. [b]1.5 equiv of aryl iodides and 3.0 eq. of aryl bromides. [c]Isolated yields with the exception of product **29** estimated by GC–MS data. % yield based on limiting reagent.

bromides and iodides were cross-coupled to bromobutane with generally good yields with only 1 mol % loading of PS and Cat. In some cases, couplings involving substituted bromobenzene compounds led to high yields (reaction 28, 85%, and reaction 30, 96%). Cross-coupling reactions involving iodo-containing aryls generally resulted in excellent yields with both electron-donating and -withdrawing substituents. Coupling of a heteroarene–halide was achieved (reaction 36, 75% yield),

DOI: 10.1021/acs.joc.6b02830
J. Org. Chem. 2017, 82, 1996–2003

which illustrates the possible range of this coupling method. Both meta- and para-functionalized aryl halides were successfully coupled. Coupling reactions between ortho-substituted aryl halides and bromobutane, however, resulted in low yields. Reaction 29 is a representative example of attempts to couple ortho-substitued aryl halides. An analysis of the reaction 29 mixture showed primarily unreacted aryl halide and dimerized alkyl halide products, with the cross-coupled product being the minor component of the gas chromatograph.

In addition to product formation, during the reactions a white precipitate continuously forms and is easily separated from the reaction mixture. Separation and recrystallization of the precipitate, followed by X-ray crystallographic analysis, showed that the precipitates were salts formed between protonated TEOA and the halide leaving groups from the consumed halocarbon substrates (Figure S31). Crystal structures of these TEOA halide salts have been previously reported.[50] These salts likely form as oxidized TEOA transfers a proton to a neutral TEOA molecule. The subsequent protonated molecule, $TEOAH^+$, then complexes halide leaving groups and forms an insoluble salt. This result shows that the TEOA reductant also acts as a "sink" for the halide leaving groups, which promotes reactivity of the substrates. This substrate reactivity promotion is typically achieved via reaction additives such as inorganic salts or strong bases as discussed in the Introduction. In addition, the insoluble salts formed between the oxidized TEOA and the halide leaving groups are easily removed from the reaction mixture and help prevent product contamination, a problem regularly encountered in both academic and industrial syntheses.[51]

Lastly, we examined the ability to scale up the PARC reactions to illustrate the ability of PARC catalysis to operate under a wide range of substrate concentrations. Reaction 37 shows that the catalytic cross-coupling of iodobenzene and bromohexane can be achieved on a gram scale in just 12 h with an excellent 96% yield. This result further illustrates the versatility of the PARC approach.

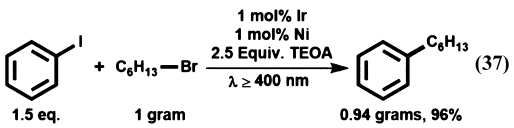

Mechanistic Considerations. The mechanism of PARC was developed with support from experimental data and results and from the previously proposed mechanism.[46] NMR spectral broadening indicates that the ground state of the nickel catalyst is paramagnetic. In addition, cyclic voltammetry studies show that the first reduction of **Cat** (Ni^{II} to Ni^{I}) occurs at $E_{1/2} = -1.06$ V vs Fc^+/Fc, and the second reduction of Cat, Ni^{I} to Ni^{0} ($E_{1/2} = -1.72$ V). For the case of the doubly reduced catalyst, Ni^0, both a d^{10} complex and the corresponding $(tpy^-)Ni^I$ complex have been proposed.[47]

Addition of bromobutane and/or iodobenzene substrate into the electrochemical solution during cyclic voltammetry experiments does not change the current response for the Ni^I/Ni^{II} couple, indicating that the Ni^I oxidation state of Cat is not active enough to react with aryl or alkyl halides. Therefore, it is believed that a second reduction of the catalyst to generate Ni^0 is necessary to initiate reactivity with the halocarbon substrates. Further reduction of Ni^I to Ni^0 generates a nickel oxidation state that is reactive toward oxidation addition of halocarbons, as evidenced by an increase in current at the second reduction wave of the catalyst during cyclic voltammetry experiments with increasing additions of halocarbons (Figure S2).

Formation of alkyl radicals from alkyl halides has been shown experimentally[52,53] and computationally.[54] To test for the possibility of sp^3-radical intermediates, the reactivity of the radical probe cyclopropylmethyl bromide was examined with our system. Formation of a radical from cyclopropylmethyl bromide should lead to a rearrangement and formation of a homoallylic radical.[55] Scheme 3 illustrates the results of the homocoupling of

Scheme 3. Radical Probe Experiment

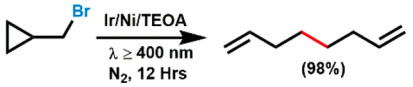

cyclopropylmethyl bromide, which resulted in 98% selectivity for the completely rearranged product. These results are consistent with the formation of alkyl radicals being formed during the proposed catalytic cycle.

To investigate the possibility of the alkyl radical being generated at one nickel center and then consumed at a different nickel center, a radical clock rearrangement experiment was performed. The cross-coupling reaction between iodobenzene and 6-bromohex-1-ene was examined at various catalyst concentrations, similar to experiments previously reported.[23,56] Formation of the hexynyl radical from 6-bromohex-1-ene can lead to rearrangement to the cyclopentylmethyl radical. The rate of rearrangement is sufficiently slow in order to observe both rearranged and unrearranged products in cross-coupling reactions. If the PARC system operates via a mechanism where an alkyl radical is generated at one nickel center and consumed at another nickel center, the observed ratio of rearranged and unrearranged products should be dependent on the concentration of catalyst. As shown in Figure 4, the ratio of products is indeed dependent on catalyst concentration, therefore, supporting a mechanism involving alkyl-radical generation.

As shown in Scheme 2, the catalytic system is not capable of forming sp^2–sp^2 dimers. This lack of reactivity toward the formation of sp^2–sp^2 carbon bonds is seen as an advantage for

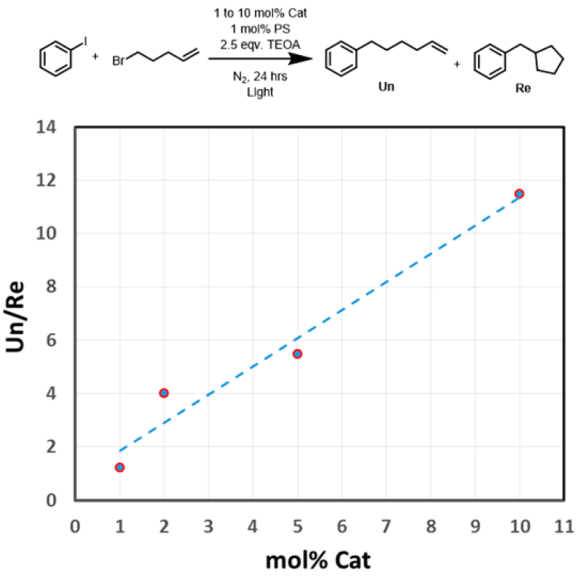

Figure 4. Ratio of unrearranged (Un) to rearrarranged (Re) product at varying catalyst loadings.

DOI: 10.1021/acs.joc.6b02830
J. Org. Chem. 2017, 82, 1996−2003

the purpose of selective sp^2-sp^3 cross-coupling. The $2e^-$ oxidative addition of the sp^2 carbon electrophile to Ni^0, however, needs to be thermodynamically and kinetically facile to compete with the alkyl dimerization reaction. Under 1:1 mixtures of iodobenzene and bromobutane, nearly a 50:50 mixture of butylbenzene (cross-coupled product) and octane (alkyl dimer product) is observed via GC–MS analysis. Hence, a slight excess of 1.5 equiv of iodobenze is required to optimize the yield of cross-coupled product and prevent alkyl dimerization. These results indicate the importance of a Ni–Ph intermediate in the catalytic cycle.

To support the claim of a Ni–Ph intermediate we performed a series of experiments to monitor the catalytic cycle with NMR spectroscopy. In an initial experiment, iodobenzene only was mixed with **Cat**, **PS**, and TEOA in acetonitrile. Aliquots of the reaction mixture were then examined by NMR spectroscopy at various time intervals.

Before light was shown on the reaction, the NMR spectrum of the mixture, shown in Figure 5a, exhibited only broad peaks in

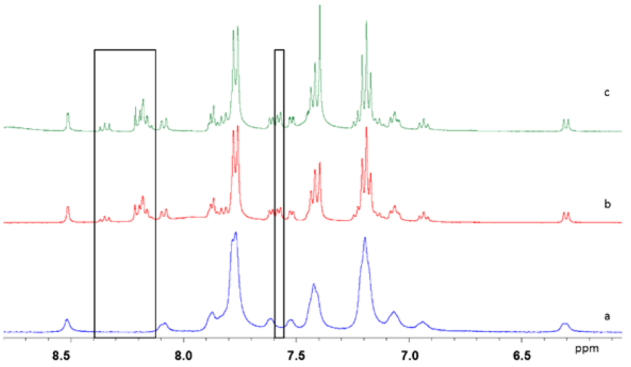

Figure 5. NMR spectra of reaction containing iodobenzene, 0.5 equiv of **Cat**, 0.25 equiv of **PS**, and 2 equiv of of TEOA in acetonitrile. (a) At time zero, before visible light irradiation. (b) After 1 h of light irradiation. New peaks appear at 7.55, 8.20, and 8.35 ppm, indicating the formation of a reaction intermediate. (c) After 3 h of irradiation.

the aromatic region attributed to the iridium photosensitizer and the iodobenzene substrate that have been broadened by the presence of the paramagnetic nickel catalyst. After 1 h of light irradiation, the original peaks in the spectrum have sharpened, and three new peaks are observed near 7.55, 8.20, and 8.35 ppm in Figure 5b. These three peaks maintain intensity from 1 to 3 h. These peaks are unique to reactions containing iodobenzene and are not observed when bromobutane is in the reaction mixture and iodobenzene has been omitted (Figure S4).

In a second experiment both iodobenzene and bromobutane were mixed with **Cat**, **PS**, and TEOA in acetonitrile. As observed with the first experiment, at time zero before light irradiation, no peaks near 7.55, 8.20, and 8.35 ppm were observed (Figure 6a). After 3 h of light irradiation, the three peaks previously observed in the iodobenzene experiment were once again observed at 7.55, 8.20, and 8.35 ppm. New NMR peaks were also observed at 7.35 and 8.55 ppm, and these peaks have been identified as signals from free pyridine, which has labialized off the nickel catalyst. The peaks at 7.55, 8.20, and 8.35 are only observed when iodobenzene is present; hence, we are proposing these peaks as support for the $(tpy)Ni^{II}(Ph)(I)$ intermediate that is essential for cross-coupling catalysis, which is analogous to previously reported reductive cross-coupling mechanisms proposed by multiple research groups.[23,45,46]

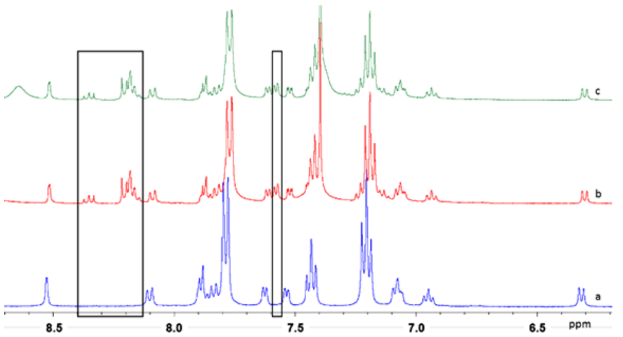

Figure 6. NMR spectra of reaction containing 1 equiv of bromobutane, 1.5 equiv of iodobenzene, 0.5 equiv of **Cat**, 0.25 equiv of PS, and 2 equiv of TEOA. (a) At time zero, before light irradiation. (b) After 3 h of light irradiation. New peaks have appeared at 7.55, 8.20, and 8.35 ppm, indicating the formation of a reaction intermediate formed between Cat and iodobenzene. (c) After 5 h of irradiation.

Another set of experiments were performed in an attempt to illustrate the importance of the Ni–Ph intermediate in the formation of the desired cross-coupled products. Under an N_2 atmosphere, 1 equiv each of $Ni^0(cod)_2$, terpyridine, pyridine, and iodobenzene were added to an acetonitrile solution and stirred at room temperature for 2 h. After 2 h, 1 equiv of PS, 1 equiv of bromobutane, and 2 equiv of TEOA were added to the solution. This solution was irradiated with visible light with stirring for an additional 2 h. GC–MS analysis of the reaction mixture shows the presence of the desired cross-coupled product (Figure S27). Formation of the desired cross-coupled product shows that adding Ph–I to the reaction mixture first, followed by addition of an alkyl halide, successfully generates products.

In an identical approach, a second experiment was performed in which under an N_2 atmosphere, 1 equiv each of $Ni^0(cod)_2$, terpyridine, pyridine, and bromobutane were added to an acetonitrile solution and stirred at room temperature for 2 h. After 2 h, 1 equiv of PS, 1 equiv of iodobenzene, and 2 equiv of TEOA were added to the solution, followed by 2 h of stirring under light irradiation. GC–MS analysis of this solution did not show the presence of the cross-coupled product, but instead only showed dimer formation (Figure S28). These results that show that the desired cross-coupled product only forms when the system is capable of first forming a Ni–Ph intermediate supports the mechanism proposed in Figure 7 and helps explain why a small excess of the aryl halide coupling partner is necessary to optimize yields.

Once the $(tpy)Ni^{II}(Ph)(I)$ intermediate is formed, it can react with the previously generated butyl radical to form a $Ni^{III}(Ph)(Bu)$ intermediate. It is postulated that the butyl radical is also generated by the Ni^0 intermediate, as shown in Figure 6. This postulation is supported by the cyclic voltammetry studies discussed above showing no response to substrate addition until the second reduction of the nickel catalyst is observed and is in agreement with the previously reported mechanism by the Lei group.[46] Reductive elimination of the cross-coupled product and return of the nickel catalyst to the Ni^I intermediate of the catalytic cycle is illustrated in the complete catalytic cycle in Figure 7, which, as a whole, is in agreement with the previously suggested mechanism.[46]

A key aspect to this catalytic mechanism is the continuous regeneration of a fully reduced Ni^0 catalyst. Reduction of the nickel catalyst is achieved by first creating an excited state of the iridium photosensitizer with visible light. The excited state PS is

DOI: 10.1021/acs.joc.6b02830
J. Org. Chem. 2017, 82, 1996–2003

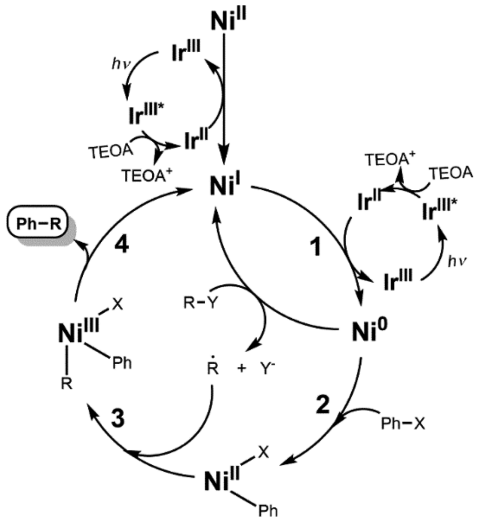

Figure 7. Proposed mechanism for photoredox-assisted reductive C−C cross-coupling.

then reductively quenched by TEOA. The fully reduced iridium PS then reduces the nickel catalyst via outersphere electron transfer. This photoredox-assisted reduction of the nickel catalyst occurs to initiate the catalytic cycle and to generate the Ni^0 intermediate.

CONCLUSIONS

Through the development and understanding of substrate reactivity trends, a methodology for performing reductive coupling reactions using visible light and photoredox events has been further established. This method was examined for aryl−alkyl C−C cross couplings and exhibited efficient catalysis with low catalyst and photosensitizer loadings (1 mol %). Experimental insight into the catalytic mechanism indicated that the nickel catalyst can be doubly reduced by a photogenerated reduced iridium photosensitizer. The doubly reduced nickel catalyst can then react with both aryl and alkyl halides through either concerted two-electron oxidative additions, as is the case with aryl halides, or via one-electron radical pathways, as is the case with alkyl halides. This difference in reactivity was utilized for efficient cross-coupling catalysis. In addition, the functional group tolerance and the ability to scale up reactions illustrates that PARC should be expandable beyond aryl−alkyl cross-couplings.

EXPERIMENTAL SECTION

Materials. Anhydrous acetonitrile (MeCN) (99.8%, water ≤50 ppm) was used for all catalysis reactions. $NiCl_2{\cdot}6H_2O$ (99.95%), 2,2′:6′,2″-terpyridine (tpy), triethanolamine (TEOA, 98+%), $[(Ir(ppy)_2)_2(Cl)_2]$, 4,4′-(di*tert*-butyl)-2,2′-bipyridine(tbpy), pyridine (py) (99%), NH_4PF_6, highly pure (>99%) halocarbons, and all solvents were used without purification. $[Ir(ppy)_2(tbpy)](PF_6)$ (**PS**) was synthesized according to literature procedures.[57,58]

Instrumental. ^1H NMR spectroscopy was performed using a 300 MHz instrument, and ^{13}C NMR was performed using a 400 MHz reference $CDCl_3$ peak for ^1H NMR defined as 7.26 ppm and as 77.33 ppm (middle peak) for ^{13}C NMR.

Gas chromatography was performed on a Rtx-5 30 m long separation column with a 0.25 mm i.d., and the oven temperature program was 50 °C for 3 min followed by a 10 °C/min ramp to 300 °C. The mass spectrometry was performed with an electron ionization of 70 eV, and the spectrometer was scanned from 450 to 50 m/z at low resolution.

Cyclic voltammetry (CV) was carried out using a 3 mm diameter glassy carbon electrode working electrode. A Pt wire (99.99%) was used as the counter electrode. The reference electrode was a saturated calomel electrode (SCE). The potential of the reference electrode was adjusted by 0.40 V for the reported potentials versus the ferrocenium/ferrocene couple (Fc^+/Fc). The glassy carbon electrode was prepared by manually polishing with 0.05 μm Alumina suspension. All solutions used for electrochemical measurements contained 0.1 M tetrabutylammonium hexafluorophosphate ($TBAPF_6$) further purified by recrystallization from ethanol and dried under vacuum at 80 °C for 24 h. Acetonitrile (99.8%, water ≤50 ppm) was used without further drying but was purged with N_2 for 5 min before measurements were performed.

A solid state light source was used as a white light source at a 10.2 W output in the visible spectrum. UV light was filtered using a 400 nm long-pass cutoff wavelength filter.

Synthesis. *[Ni(tpy)Cl]Cl.* $NiCl_2{\cdot}6H_2O$ (103 mg, 0.43 mmol) was taken in 10 mL of ethanol (EtOH) and heated to reflux. Terpyridine solution (100 mg, 0.43 mmol) in 5 mL of ethanol was added dropwise to the refluxing solution. The reaction mixture became cloudy with the addition of terpyridine and was further refluxed for another 1 h. The final product, a green solid precipitate, was collected by filtration followed by several washes with ethanol and diethyl ether. Yield: 154 mg (0.42 mmol, ~98%). Anal. Calcd for $Ni_1C_{15}H_{11}N_3{\cdot}H_2O$: C, 47.30; H, 3.44; N, 11.03. Found: C, 47.43; H, 3.28; N, 10.86.

$[(Ni(tpy)(py))_2(\mu\text{-}Cl)_2](PF_6)_2$. [Ni(tpy) (Cl)](Cl) (100 mg, 0.27 mmol) was taken in 10 mL of ethanol. Pyridine (24 μL (0.3 mmol), excess) was added dropwise to the stirring suspension of [Ni(tpy)-(Cl)](Cl). The reaction mixture became a green transparent solution after 30 min of stirring. Addition of excess solid NH_4PF_6 to the cold reaction mixture yielded a pale green precipitate. The green product was collected by filtration followed by several washes with ethanol and diethyl ether. Single crystals were grown from MeCN solution by slow-diffusion with diethyl ether. The product was characterized by crystallography, and crystallographic data are provided in the SI. Yield: 143 mg (0.13 mmol). Anal. Calcd for $Ni_2C_{40}H_{32}N_8Cl_2P_2F_{12}$: C, 43.56; H, 2.92; N, 10.16. Found: C, 43.55; H, 3.01; N, 9.97.

*$[Ni(tpy)\ (py)\ (CH_3CN)_2](PF_6)_2$ (**Cat**).* [Ni(tpy) (Cl)](Cl) (100 mg, 0.27 mmol) was taken in 10 mL of ethanol. Pyridine (24 μL (0.3 mmol), excess) was added slowly until the reaction mixture became a green transparent solution in 30 min. Acetonitrile (10 mL) was added, followed by addition of excess solid NH_4PF_6 until the solution became opaque. The resulting white solid was filtered and discarded. The remaining solvent of a purple solution was then removed via rotary evaporation. The resulting solid was then sonicated in EtOH to remove excess NH_4PF_6, and the remaining solid was filtered and dried under reduced pressure to yield a gray solid. Crystallographic data are provided in the SI. Yield: 194 mg (0.26 mmol, 96%). Anal. Calcd for $NiC_{24}H_{22}N_6P_2F_{12}$: C, 38.79; H, 2.98; N, 11.31. Found: C, 39.06; H, 2.72; N, 11.36.

General Procedure for Photoassisted Reductive Coupling Reactions. Solution preparations were performed inside a N_2-filled glovebox to confirm inert atmosphere. Vials were sealed in the glovebox, removed from the glovebox, and performed on the benchtop in closed vials. For a typical experiment, 3.0 mg (3.2×10^{-6} mols) of **PS**, 2.4 mg (3.2×10^{-6} mols) of **Cat**, and 106 μL (0.8×10^{-3} mols) of TEOA were mixed with 0.32×10^{-3} mol of substrate (100 times that of the catalyst or the photosensitizer) in 4 mL of anhydrous acetonitrile in a 12 mL glass vial with TFE/SIL O/T cap. The catalytic solution was stirred under a white light source passed through a long-pass 400 nm cutoff filter for a period of 12−18 h. During the irradiation, a fan was used to prevent heating of the vials on the stir plate. Monitoring the temperature during the reaction showed the reactions were performed at a temperature range of 23−28 °C. The products were purified by column chromotography using either diethyl ether or pentane or pentane/diethyl ether or hexane or hexane/ethyl acetate mixture as eluent.

Spectroscopic characterization of all products can be found in the Supporting Information. Data match previously reported data for all previously reported compounds.

DOI: 10.1021/acs.joc.6b02830
J. Org. Chem. 2017, 82, 1996−2003

■ ASSOCIATED CONTENT

Supporting Information

The Supporting Information is available free of charge on the ACS Publications website at DOI: 10.1021/acs.joc.6b02830.

X-ray data for **Cat**, Ni-2, and $TEOAH^+Br^-$ (CIF)

^1H,^{13}C NMR product spectra, crystal structures, cyclic voltammogram of **Cat**, UV−vis of **Cat** (PDF)

■ AUTHOR INFORMATION

Corresponding Author

*E-mail: vannucci@mailbox.sc.edu.

ORCID

Aaron K. Vannucci: 0000-0003-0401-7208

Notes

The authors declare no competing financial interest.

■ ACKNOWLEDGMENTS

The authors gratefully acknowledge support for this work by the University of South Carolina.

■ REFERENCES

(1) Shi, W.; Liu, C.; Lei, A. *Chem. Soc. Rev.* **2011**, *40*, 2761−2776.
(2) Prier, C. K.; Rankic, D. A.; MacMillan, D. W. *Chem. Rev.* **2013**, *113*, 5322−5363.
(3) Everson, D. A.; Weix, D. J. *J. Org. Chem.* **2014**, *79*, 4793−4798.
(4) Gu, J.; Wang, X.; Xue, W.; Gong, H. *Org. Chem. Front.* **2015**, *2*, 1411−1421.
(5) Cherney, A. H.; Kadunce, N. T.; Reisman, S. E. *Chem. Rev.* **2015**, *115*, 9587−9652.
(6) Terao, J.; Kambe, N. *Acc. Chem. Res.* **2008**, *41*, 1545−1554.
(7) Jana, R.; Pathak, T. P.; Sigman, M. S. *Chem. Rev.* **2011**, *111*, 1417−1492.
(8) Weix, D. J. *Acc. Chem. Res.* **2015**, *48*, 1767−1775.
(9) Everson, D. A.; Jones, B. A.; Weix, D. J. *J. Am. Chem. Soc.* **2012**, *134*, 6146−6159.
(10) Yu, X.; Yang, T.; Wang, S.; Xu, H.; Gong, H. *Org. Lett.* **2011**, *13*, 2138−2141.
(11) Xu, H.; Zhao, C.; Qian, Q.; Deng, W.; Gong, H. *Chem. Sci.* **2013**, *4*, 4022−4029.
(12) Dai, Y.; Wu, F.; Zang, Z.; You, H.; Gong, H. *Chem. - Eur. J.* **2012**, *18*, 808−812.
(13) Gong, H.; Andrews, R. S.; Zuccarello, J. L.; Lee, S. J.; Gagné, M. R. *Org. Lett.* **2009**, *11*, 879−882.
(14) Wang, S.; Qian, Q.; Gong, H. *Org. Lett.* **2012**, *14*, 3352−3355.
(15) Wang, X.; Wang, S.; Xue, W.; Gong, H. *J. Am. Chem. Soc.* **2015**, *137*, 11562−11565.
(16) Molander, G. A.; Wisniewski, S. R.; Traister, K. M. *Org. Lett.* **2014**, *16*, 3692−3695.
(17) Anka-Lufford, L. L.; Prinsell, M. R.; Weix, D. J. *J. Org. Chem.* **2012**, *77*, 9989−10000.
(18) Shrestha, R.; Dorn, S. C.; Weix, D. J. *J. Am. Chem. Soc.* **2013**, *135*, 751−762.
(19) Arendt, K. M.; Doyle, A. G. *Angew. Chem., Int. Ed.* **2015**, *54*, 9876−9880.
(20) Cherney, A. H.; Kadunce, N. T.; Reisman, S. E. *J. Am. Chem. Soc.* **2013**, *135*, 7442−7445.
(21) Cherney, A. H.; Reisman, S. E. *J. Am. Chem. Soc.* **2014**, *136*, 14365−14368.
(22) Kadunce, N. T.; Reisman, S. E. *J. Am. Chem. Soc.* **2015**, *137*, 10480−10483.
(23) Biswas, S.; Weix, D. J. *J. Am. Chem. Soc.* **2013**, *135*, 16192−16197.
(24) Ren, Q.; Jiang, F.; Gong, H. *J. Organomet. Chem.* **2014**, *770*, 130−135.
(25) Wang, L.; Zhang, Y.; Liu, L.; Wang, Y. *J. Org. Chem.* **2006**, *71*, 1284−1287.
(26) Kuroboshi, M.; Waki, Y.; Tanaka, H. *J. Org. Chem.* **2003**, *68*, 3938−3942.
(27) Durandetti, M.; Nédélec, J.-Y.; Périchon, J. *Org. Lett.* **2001**, *3*, 2073−2076.
(28) Durandetti, M.; Périchon, J.; Nédélec, J.-Y. *Tetrahedron Lett.* **1997**, *38*, 8683−8686.
(29) Durandetti, M.; Périchon, J. *Synthesis* **2004**, *2004*, 3079−3083.
(30) Prinsell, M. R.; Everson, D. A.; Weix, D. J. *Chem. Commun.* **2010**, *46*, 5743−5745.
(31) Netherton, M. R.; Fu, G. C. *Adv. Synth. Catal.* **2004**, *346*, 1525−1532.
(32) Cong, H.; Fu, G. C. *J. Am. Chem. Soc.* **2014**, *136*, 3788−3791.
(33) Hironaka, K.; Fukuzumi, S.; Tanaka, T. *J. Chem. Soc., Perkin Trans. 2* **1984**, 1705−1709.
(34) Kern, J.-M.; Sauvage, J.-P. *J. Chem. Soc., Chem. Commun.* **1987**, 546−548.
(35) Tellis, J. C.; Primer, D. N.; Molander, G. A. *Science* **2014**, *345*, 433−436.
(36) Zuo, Z.; Ahneman, D. T.; Chu, L.; Terrett, J. A.; Doyle, A. G.; MacMillan, D. W. C. *Science* **2014**, *345*, 437−440.
(37) Tellis, J. C.; Kelly, C. B.; Primer, D. N.; Jouffroy, M.; Patel, N. R.; Molander, G. A. *Acc. Chem. Res.* **2016**, *49*, 1429−1439.
(38) Jouffroy, M.; Primer, D. N.; Molander, G. A. *J. Am. Chem. Soc.* **2016**, *138*, 475−478.
(39) Jeffrey, J. L.; Petronijević, F. R.; MacMillan, D. W. C. *J. Am. Chem. Soc.* **2015**, *137*, 8404−8407.
(40) Terrett, J. A.; Cuthbertson, J. D.; Shurtleff, V. W.; MacMillan, D. W. C. *Nature* **2015**, *524*, 330−334.
(41) Noble, A.; McCarver, S. J.; MacMillan, D. W. C. *J. Am. Chem. Soc.* **2015**, *137*, 624−627.
(42) Patel, N. R.; Molander, G. A. *J. Org. Chem.* **2016**, *81*, 7271−7275.
(43) Joe, C. L.; Doyle, A. G. *Angew. Chem., Int. Ed.* **2016**, *55*, 4040−4043.
(44) Corcoran, E. B.; Pirnot, M. T.; Lin, S.; Dreher, S. D.; DiRocco, D. A.; Davies, I. W.; Buchwald, S. L.; MacMillan, D. W. C. *Science* **2016**, *353*, 279−283.
(45) Zhang, P.; Le, C. C.; MacMillan, D. W. C. *J. Am. Chem. Soc.* **2016**, *138*, 8084−8087.
(46) Duan, Z.; Li, W.; Lei, A. *Org. Lett.* **2016**, *18*, 4012−4015.
(47) Ciszewski, J. T.; Mikhaylov, D. Y.; Holin, K. V.; Kadirov, M. K.; Budnikova, Y. H.; Sinyashin, O.; Vicic, D. A. *Inorg. Chem.* **2011**, *50*, 8630−8635.
(48) Goldup, S. M.; Leigh, D. A.; McBurney, R. T.; McGonigal, P. R.; Plant, A. *Chem. Sci.* **2010**, *1*, 383−386.
(49) Tsai, K. Y.-D.; Chang, I. J. *Inorg. Chem.* **2017**, *56*, 693−696.
(50) Laszio, P.; Pal, H.; Laszio, N.; P, B. V. *Kem. Koz.* **1991**, *73*, 279.
(51) Garrett, C. E.; Prasad, K. *Adv. Synth. Catal.* **2004**, *346*, 889−900.
(52) Breitenfeld, J.; Ruiz, J.; Wodrich, M. D.; Hu, X. *J. Am. Chem. Soc.* **2013**, *135*, 12004−12012.
(53) Schley, N. D.; Fu, G. C. *J. Am. Chem. Soc.* **2014**, *136*, 16588−16593.
(54) Breitenfeld, J.; Wodrich, M. D.; Hu, X. *Organometallics* **2014**, *33*, 5708−5715.
(55) Phapale, V. B.; Buñuel, E.; García-Iglesias, M.; Cárdenas, D. J. *Angew. Chem., Int. Ed.* **2007**, *46*, 8790−8795.
(56) Kinney, R. J.; Jones, W. D.; Bergman, R. G. *J. Am. Chem. Soc.* **1978**, *100*, 7902−7915.
(57) DiSalle, B. F.; Bernhard, S. *J. Am. Chem. Soc.* **2011**, *133*, 11819−11821.
(58) Paul, A.; Das, N.; Halpin, Y.; Vos, J. G.; Pryce, M. T. *Dalton Trans.* **2015**, *44*, 10423−10430.

DOI: 10.1021/acs.joc.6b02830
J. Org. Chem. 2017, 82, 1996−2003